Calibration and Interpretation of STIS Imaging Mode Fluxes

Charles R. Proffitt
Science Programs, Computer Sciences Corporation, and Space Telescope Science Institute

Introduction

While primarily a spectroscopic instrument, STIS also had a number of imaging modes, many of which provided unique capabilities, especially in the ultraviolet. However, most of the STIS imaging modes also had very wide, non-standard passbands, making the calibration and interpretation of STIS imaging data especially challenging. Here we describe the methods used to derive the adopted throughput curves, zero points, and aperture corrections for these modes and also estimate the remaining uncertainties in these quantities. The wide, non-standard passbands of STIS imaging modes also present special challenges when comparing to observations in other photometric systems. To aid in interpretation, we discuss the relationship between STIS magnitudes and colors and those of other common photometric system.

STIS Imaging Zero Points and Time Dependence.

The STIS instrument has 3 detectors, a CCD sensitive from ~ 2000 to 10,300 Å, a Cs_2Te Multi-Anode Microchannel Array (MAMA) detector (1600 to 3100 Å) and a solar-blind CsI MAMA (1150 to 1700 Å). Sensitivities of these detectors have varied over time. For a given detector these changes depend on λ, but appear to be independent of the mode. So for imaging observations we will adopt the same time dependence that was determined for the 1st order spectroscopic modes (Stys et al. 2004, STIS ISR 2004-04). This leads to considerable color dependence of the sensitivity change with time. In Figure 1 we give examples of the predicted sensitivity changes for stars of different colors at 380 day intervals over the 7+ year operational life of STIS.

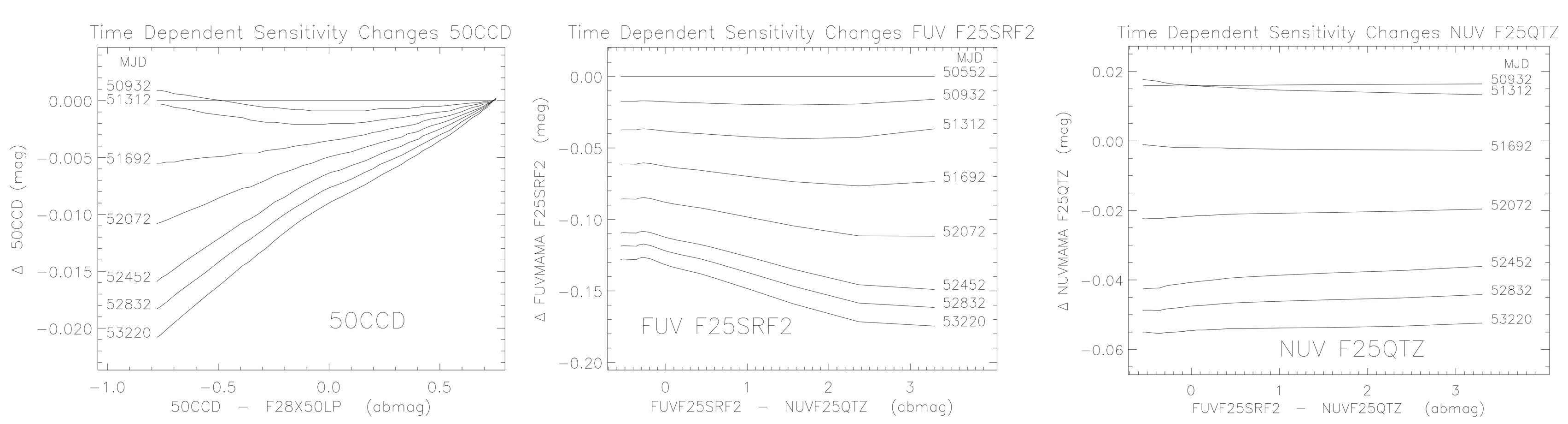

Figure 1: Predicted changes in sensitivity as a function of time and color for selected STIS modes are shown at 380 day intervals over the operational lifetime of the STIS instrument.

The available detector/imaging filter combinations are summarized in Table 1 for a time near the beginning of STIS operations. The corresponding keywords in individual STIS image headers take into account the time dependent sensitivity changes, and contain values appropriate for the actual date of each observation.

Table 1: STIS Imaging Mode Zero Points on MJD 50552 (April 14, 1997)

FILTER	PHOTPLAM	PHOTFLAM	PHOTBW	STmag	ABmag	VEGAmag
CCD						
50CCD	5733.2271	9.951026e-20	1840.0298	26.405	26.305	26.061
F28X50LP	7216.7495	1.639466e-19	1139.8442	25.863	25.264	24.990
F28X50OII	3738.0562	4.689609e-17	24.1437	19.722	20.551	19.724
F28X50OIII*	5005.7637	1.336786e-16	2.6480	18.585	18.780	18.864
F25ND3	6314.8350	4.507867e-17	1987.7416	19.765	19.455	19.197
F25ND5	7010.8442	7.399737e-15	2000.8271	14.227	13.690	13.401
NUV MAMA						
25MAMA	2263.3516	4.986097e-18	508.3389	22.156	24.074	22.357
F25SRF2	2304.0161	5.566799e-18	478.3638	22.036	23.916	22.238
F25QTZ	2357.8860	5.922293e-18	420.1680	21.969	23.798	22.161
F25CIII	2010.9514	4.404841e-16	163.1308	17.290	19.465	17.742
F25CN182	2006.9155	5.932350e-17	285.6461	19.467	21.646	19.868
F25MGII	2873.8157	2.014965e-16	248.9775	18.139	19.539	18.151
F25CN270	2722.8352	3.923132e-17	121.8445	19.916	21.433	19.951
F25ND3	2358.4878	4.460867e-15	553.1555	14.776	16.605	14.931
F25ND5	2630.3911	3.358502e-12	623.3374	7.585	9.177	7.660
FUV MAMA						
25MAMA	1374.3839	2.102782e-17	137.5971	20.593	23.595	20.732
F25SRF2	1457.3762	3.800120e-17	120.4711	19.951	22.825	20.447
F25QTZ	1595.0404	1.036147e-16	96.7376	18.861	21.540	19.516
F25LYA	1243.0822	1.047616e-15	61.7426	16.350	19.569	14.915
F25ND3	1376.0492	2.146214e-14	134.2651	13.071	16.070	13.229
F25ND5	1385.0936	3.011165e-11	141.6614	5.203	8.188	5.383

* Parameters given here for the OIII filter exclude the red-leak.

Here PHOTPLAM is the pivot λ, PHOTFLAM is the flux (ergs/cm^2/s/Å) of a flat spectrum that produces 1 cnt/sec in each mode, and PHOTBW the passband RMS width. See the "SYNPHOT User's Guide" (Laidler et al. 2005) for detailed definitions of these parameters.

Determination of Absolute Throughputs

Since STIS is a spectrograph as well as an imaging instrument, the relative throughputs of different filters as a function of wavelength were easily determined by comparing filtered and unfiltered spectra of the same stars. To determine the wavelength dependent throughput of each detector's unfiltered mode, a small number of stars with well measured SEDs and spanning a wide range of colors were observed. Deep images were taken in several filters to allow aperture corrections to be measured to large radii.The pre-launch estimates of the unfiltered mode throughputs vs. wavelength were then adjusted to match the observed count rates for each filter and target.

For CCD imaging modes, the details of this calibration were presented in Proffitt 2004 (STIS ISR 2004-05). The unfiltered CCD throughput at long wavelengths had to be increased by up to 18% above prelaunch estimates. In addition, the scattering of light into an extended red halo put up to 20% of the flux at distances from the image center > 0.5". Wavelength dependent aperture corrections were also estimated using these data.

For MAMA broadband clear, strontium fluoride, and quartz filters, existing standard stars were too bright, and to provide well calibrated standards long-slit STIS G140L, G230L, and G430L spectra were taken of a number of hot HB stars in the globular cluster NGC 6681. This cluster was also used as the primary calibration object for the long term monitoring of the MAMA imaging stability, and so copious images of these same stars are available in most MAMA imaging modes. Details of the MAMA imaging absolute flux calibration are given in Proffitt et al. 2003 (STIS ISR 2003-01).

Relationship of STIS CCD to other Photometric Systems

Comparing the STIS CCD throughput curves to standard broadband Johnson filters shows that the STIS passbands (Figure 2) extend to significantly longer and shorter wavelengths than does the $UBVR_cI_c$ system, and any transformation between STIS and other broadband photometric systems will depend strongly on the details of the SED Figure 3.

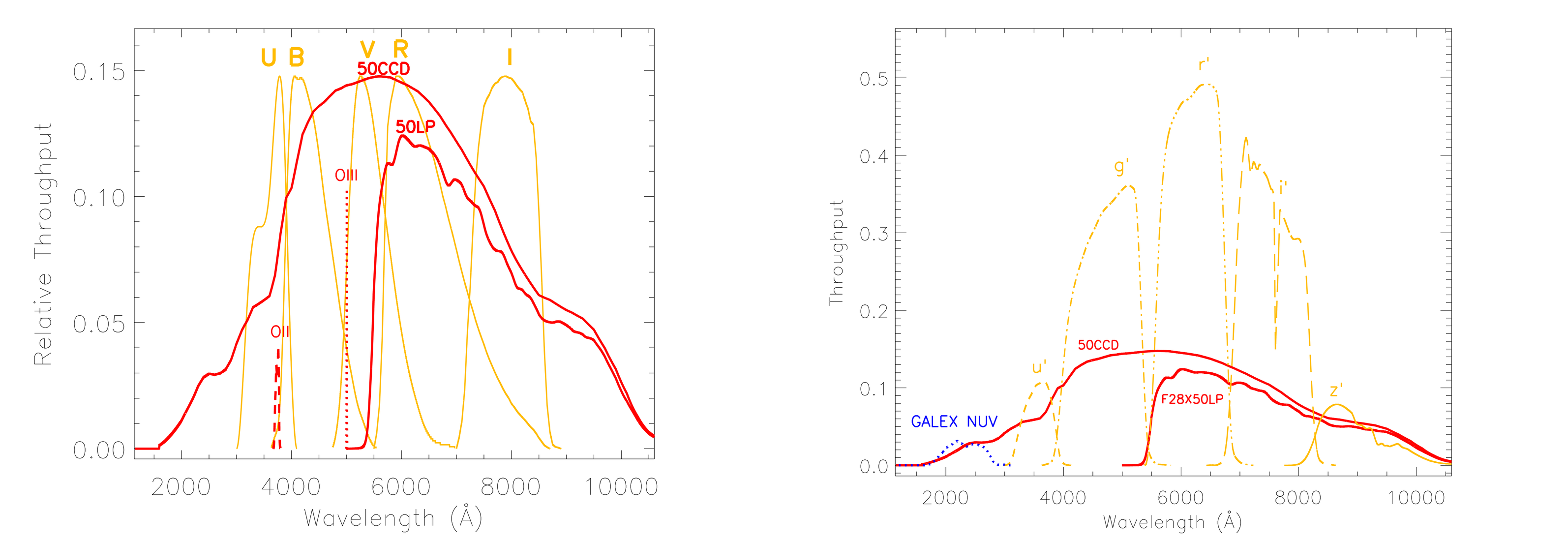

Figure 2: On the left, the throughput of the STIS CCD modes (red) is compared with the scaled throughputs of the standard $UBVR_cI_c$ photometric system (orange). In the right figure, STIS throughputs are compared with SDSS *u'g'r'i'z'* and GALEX NUV throughput curves.

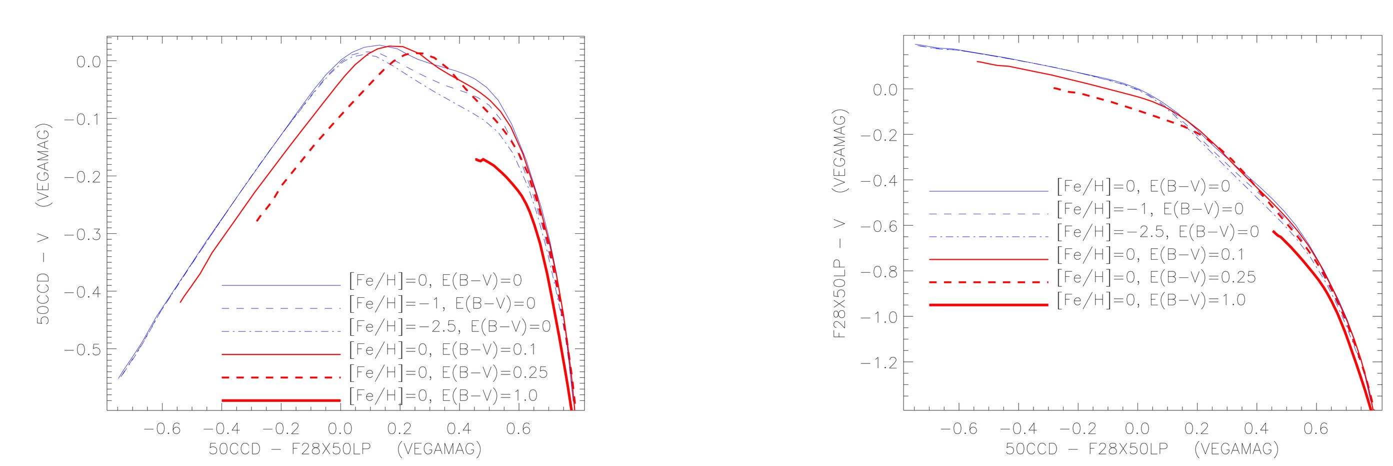

Figure 3: Relation between STIS 50CCD (left) and F28X50LP (right) magnitudes and Johnson V band as a function of color for series of Kurucz main-sequence models, ranging in T_{eff} from 50000 to 3500 K, and with a variety of metallicities and reddenings.

Color-color transforms are somewhat tighter, but still show considerable dependency on the details of the SEDs.

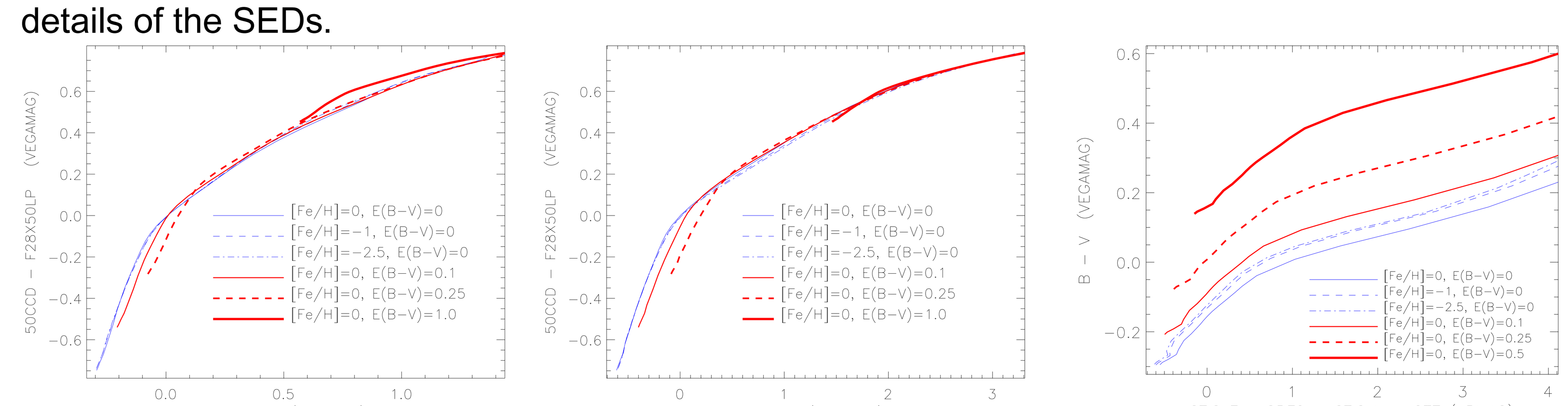

Figure 4: Relationship between STIS and Johnson colors for a variety of Kurucz main-sequence model sequences.

The combined long wavelength filters of Gunn type photometric systems, such as that used for the Sloane Digital Sky Survey (York et al., 2000), provide a better match to the F28X50LP filter throughput (right hand panel of Figure 2). While no ground based system can reach wavelengths as short as the unfiltered STIS CCD, the short-wavelength cutoff is close to the GALEX NUV band. This makes it possible to use SDSS photometry to robustly predict STIS CCD magnitudes. This may be useful to place STIS observations in the context of these broader surveys or to easily use synthetic colors calculated for these systems when interpreting STIS imaging observations.

If, for the Kurucz models considered above, we fit the STIS fluxes as a sum of the measured AB fluxes, $M_{AB}(STIS) = -2.5\log\left(\sum_f c_i 10^{((-M_{AB}(f))/2.5)}\right)$,we find the coefficients in Table 2.

Table 2: Coefficients to convert SDSS/Galex magnitudes to STIS 50CCD and F28X50LP AB magnitudes

Target STIS color	Coefficients of Fit						
	GALEX NUV	u'	g'	r'	i'	z'	RMS residuals
F28X50LP				0.527	0.250	0.224	0.0025
50CCD		0.304	0.307	0.131	0.218	0.071	0.019
50CCD	0.070	0.147	0.348	0.209	0.140	0.091	0.0020

Comparison of MAMA and GALEX Passbands

STIS has a variety of broadband UV imaging filters for use with the MAMAs. No particular combination of the available choices was adopted as a standard color, although the FUV SRF2 and the NUV QTZ were the most commonly used combinations. However, the GALEX mission (Martin et al. 2005) will survey the entire sky in passbands similar to those available with STIS, and this suggests that the GALEX passbands may become such a "standard" vacuum UV color.

In Figure 5 and Figure 6, we compare STIS MAMA and GALEX imaging passbands and colors. For unreddened stars, relatively tight transformations between these systems might be defined, but when extinction becomes substantial, the differences in wavelength cutoffs for these filters have large effects. Any attempts to cross-calibrate STIS and GALEX UV imaging magnitudes will have to pay close attention to the details of the SEDs.

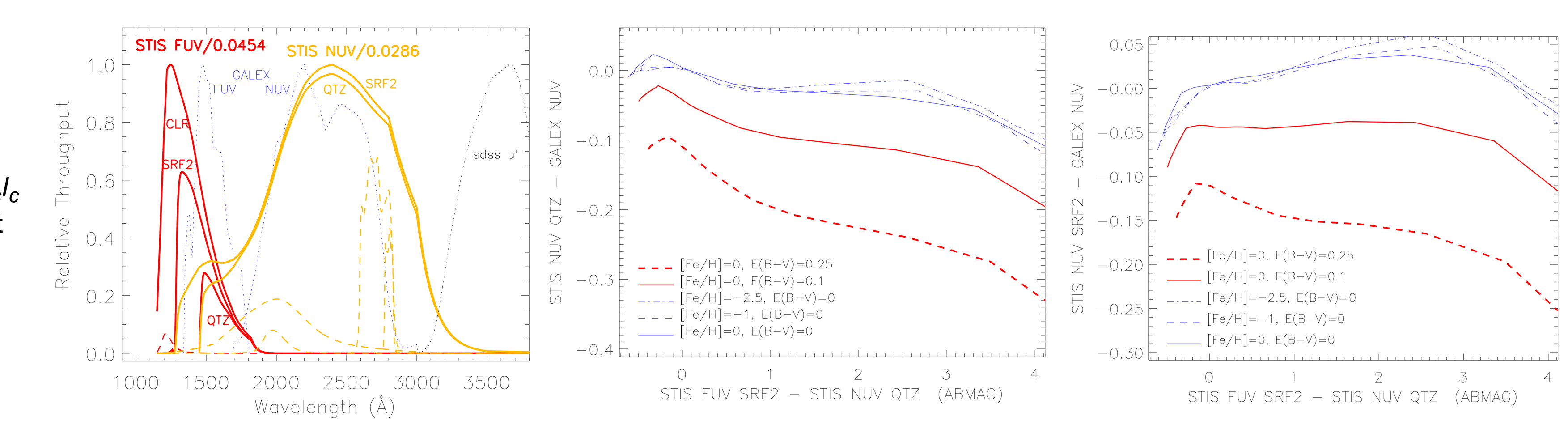

Figure 5: On the left, we compare the STIS FUV (red) and NUV (orange) MAMA passbands to those of GALEX (blue). The other panels show how STIS broadband NUV SRF2 and NUV QTZ magnitudes compare to those measured with GALEX, for Kurucz models of a variety of metallicities and reddenings. We make these comparisons as a function of the STIS FUV SRF2 – STIS NUV QTZ ABMAG color. The third panel of Figure 4 showed the relation between this color and Johnson *B–V.*

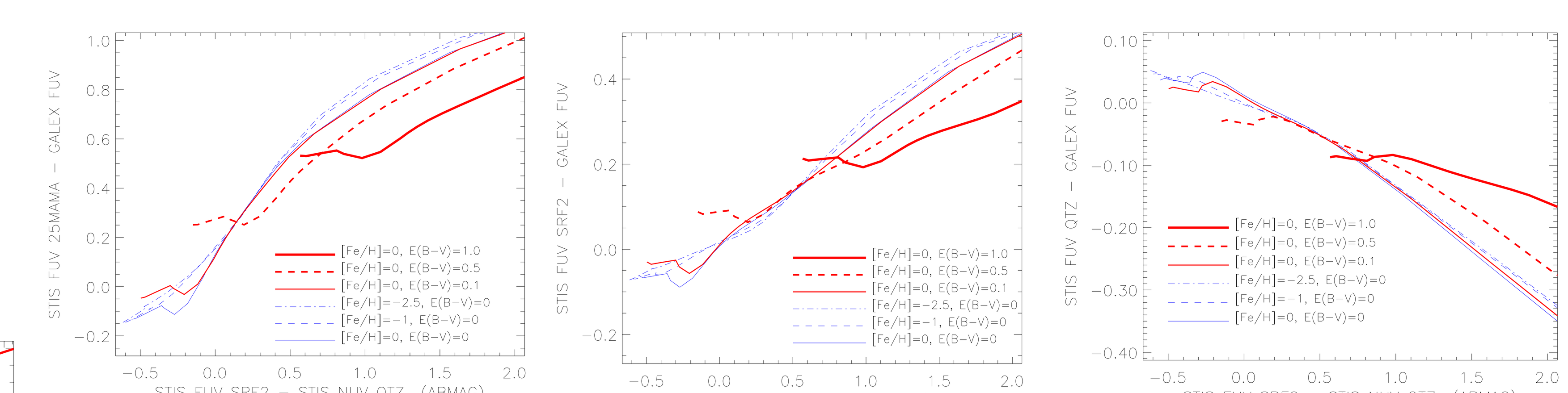

Figure 6: Comparison between STIS FUV MAMA broadband magnitudes and GALEX magnitudes as a function of color for Kurucz models with a variety of metallicities and reddenings.

References

Laidler et al, 2005, Synphot Data Users Guide (Baltimore, STScI)
Martin, D. C., et al. 2005, ApJ, 610, 1
Proffitt, C. R. 2004, STIS ISR 2004-05, (Baltimore, STScI)
Proffitt, C. R., Brown, T. M., Mobasher, B., & Davies, J. 2003, STIS ISR 2003-01 (Baltimore, STScI)
Stys, D. J., Bohlin, R. C., & Goudfrooij, P. 2004, STIS ISR 2004-04 (Baltimore, STScI)
York, D. G., et al. 2000, AJ, 120, 157